



Trade Science Inc.

Materials Science

An Indian Journal

Full Paper

MSAIJ, 8(7), 2012 [263-270]

Effect of temperature on electrical conductivity and dielectric properties for manganese substituted lithium ferrite

S.A.Mazen, N.I.Abu-Elsaad*

Magnetic Semiconductor Laboratory, Physics Department, Faculty of Science, Zagazig University, Zagazig, (EGYPT)

E-mail: nagwa.ibrahim@yahoo.com

Received: 26th January, 2012 ; Accepted: 26th February, 2012

ABSTRACT

Manganese substituted lithium-ferrite with the general formula $\text{Li}_{0.5-0.5x}\text{Mn}_x\text{Fe}_{2.5-0.5x}\text{O}_4$ (where $x = 0.0, 0.1, 0.3, 0.5, 0.7, 0.9$ and 1.0) were synthesized by the standard ceramic technique. The variation of dc and ac conductivities has been reported as a function of temperature from room temperature 293K up to 970K in static air. Ac measurements were carried out over a wide range of frequencies from 100Hz up to 1MHz. The variation in σ at room temperature with composition indicates that the conductivity initially increases up to 0.5 and then decreases with further addition in Mn content. The activation energy of conduction mechanism decreases from 0.68eV to 0.34eV. The electrical conduction in this ferrite is explained on the basis of the hopping mechanism. Dielectric properties such as dielectric loss tangent $\tan \delta$ and dielectric constant ϵ' have been measured. The dielectric behaviour is explained by using the mechanism of polarization process, which is correlated to that of exchange interaction.

© 2012 Trade Science Inc. - INDIA

KEYWORDS

Ferrite;
Conductivity;
Dielectric;
Li-Mn ferrite.

INTRODUCTION

Spinel ferrites are one of the most important classes of magnetic ceramic materials owing to their interesting applications. In the spinel structure, the magnetic ions are distributed among two different sub-lattice sites, tetrahedral (A) and octahedral (B) sites. The physical properties of ferrites depend on chemical composition, type and amount of dopant, method of preparation, magnetic interaction and cation distribution in the two sub-lattices^[1,2].

Lithium ferrite $\text{Li}_{0.5}\text{Fe}_{2.5}\text{O}_4$ is a well known ferrimagnetic composition with an inverse spinel structure in which

the tetrahedral sites (A) are occupied by Fe^{3+} ions and the octahedral sites (B) by Li^+ and Fe^{3+} ions^[3]. Lithium ferrite considered as a unique member of the spinel class of ferrimagnets and is dominating the field of microwave applications and memory core applications because of its rectangular and square hysteresis loop characteristics, large value of saturation magnetization, low microwave dielectrics and low costs^[4]. Several studies on Li-ferrite have been discussed recently by many authors^[5-7]

Manganese ferrite MnFe_2O_4 was originally thought to be inverse but was later found to be nearly normal, about 80% manganese ions occupy the tetrahedral (A-sites) and 20% occupy the octahedral (B-sites)^[8]. Man-

Full Paper

ganesse ferrite is a common ferrite material being widely used in microwave and magnetic recording applications due to its high permeability and low eddy current losses^[9]. It has attracted considerable attention due to its broad applications in several technological fields including electronic devices, ferro-fluids, magnetic drug delivery, microwave devices and high-density information storage^[10,11]. Many studies about structural, electrical and magnetic properties of Mn-ferrite have been reported^[12-14]

Several studies^[15-17] have been reported with addition of divalent, trivalent and tetravalent ions in appropriate amount into formula unit $\text{Li}_{0.5}\text{Fe}_{2.5}\text{O}_4$ in order to optimize the numerous properties of interest like electric and dielectric. However, no reports have been found in the literature regarding the dielectric properties of manganese substituted lithium ferrite prepared by conventional double sintering ceramic technique as a function of elevated temperature.

Therefore, in this report we have undertaken a systematic study of the electrical conductivity and dielectric properties of Li-Mn ferrite over a wide range of temperature and frequency.

EXPERIMENTAL TECHNIQUE

The investigated samples of Li-Mn ferrite having the general formula $\text{Li}_{0.5}\text{Fe}_{2.5-x}\text{Mn}_x\text{O}_4$ (where $x = 0.0, 0.1, 0.3, 0.5, 0.7, 0.9$ and 1.0) were synthesized by the standard ceramic technique from mixing the pure reagents (Fe_2O_3 , Li_2CO_3 and MnO). The weighted materials were mixed and then grounded to a very fine powder using ball milling machine (model puluer isette 6). The mixture of each composition was pre-sintered at 750°C for 10 h. The samples were pressed in a disk-

shaped form of 13-mm diameter, and 3-5-mm thickness and finally sintered at 1200°C for 10 hrs. The samples were polished and coated by silver paste for the electrical conductivity measurements. Electrical conductivity of the investigated samples was measured in a wide range of temperature from room temperature 300K up to 950K in static air by the two probes method using (AC-DC bridge type FLUKA model PM6306). Digital temperature indicator (model Pro'sKit 03-9303) with resolution 1K, connected with a standard K-type thermocouple was used to measure the temperature from room temperature up to 950K.

RESULTS AND DISCUSSION

Dc and Ac electrical conductivity

The variation of dc and ac conductivities with temperature of the above investigated composition of $\text{Li}_{0.5-0.5x}\text{Mn}_x\text{Fe}_{2.5-0.5x}\text{O}_4$ has been studied. The measurements were carried out over a wide range of temperature from 300 up to 950K; the ac electrical conductivity was measured in the range of frequencies from 10^2 to 10^6 Hz. The logarithm of conductivity ($\ln \sigma$) as a function of reciprocal temperature (T^{-1}) is shown in Figure 1. The conductivity of both dc and ac show an increase with increasing temperature. Accordingly, the Li-Mn ferrite shows a semiconducting trend, which is commonly seen in most ferrites, and can be represented by Arrhenius relationship:

$$\sigma = \sigma_0 \exp\left(\frac{-E_\sigma}{KT}\right) \quad (1)$$

where σ is the specific conductivity, σ_0 the temperature-dependent constant, E_σ represents the activation energy, K the Boltzman's constant and T the absolute

TABLE 1 : The activation energy E_σ from dc and ac conductivity measurements for $\text{Li}_{0.5-0.5x}\text{Mn}_x\text{Fe}_{2.5-0.5x}\text{O}_4$ at different frequencies.

x	Dc		10 ² Hz		10 ³ Hz		10 ⁴ Hz		10 ⁵ Hz		5x10 ⁵ Hz		10 ⁶ Hz	
	Ferri	Para	Ferri	Para	Ferri	Para	Ferri	Para	Ferri	Para	Ferri	Para	Ferri	Para
0.0	0.67	-	0.65	-	0.63	-	0.62	-	0.56	-	0.46	-	0.44	-
0.1	0.52	0.61	0.51	-	0.51	-	0.50	-	0.47	-	0.44	-	0.42	-
0.3	0.44	0.47	0.45	-	0.44	-	0.44	-	0.42	-	0.40	-	0.38	-
0.5	0.41	0.54	0.41	0.53	0.40	0.53	0.37	0.53	0.34	0.48	0.33	-	0.31	-
0.7	0.41	0.59	0.41	0.58	0.39	0.58	0.35	0.58	0.31	0.56	0.30	0.39	0.30	0.32
0.9	0.40	0.53	0.39	0.52	0.37	0.52	0.34	0.52	0.31	0.51	0.29	0.41	0.29	-
1.0	0.44	0.56	0.44	0.56	0.43	0.56	0.39	0.56	0.33	0.55	0.37	0.49	0.37	0.42

temperature. The values of the activation energy are tabulated in TABLE 1 for two different regions, ferromagnetic and paramagnetic (i.e. for $T < T_C$ and $T > T_C$, respectively).

According to Figure 1, the behaviour of $\ln \sigma$ versus

T^{-1} can be divided into three main regions: the first region I for $T < T_L$, which appeared only for $x=0.0$ and 0.1 , the second region II (intermediate-temperature region which lies between T_L and T_H) and the third region III for $T > T_H$.

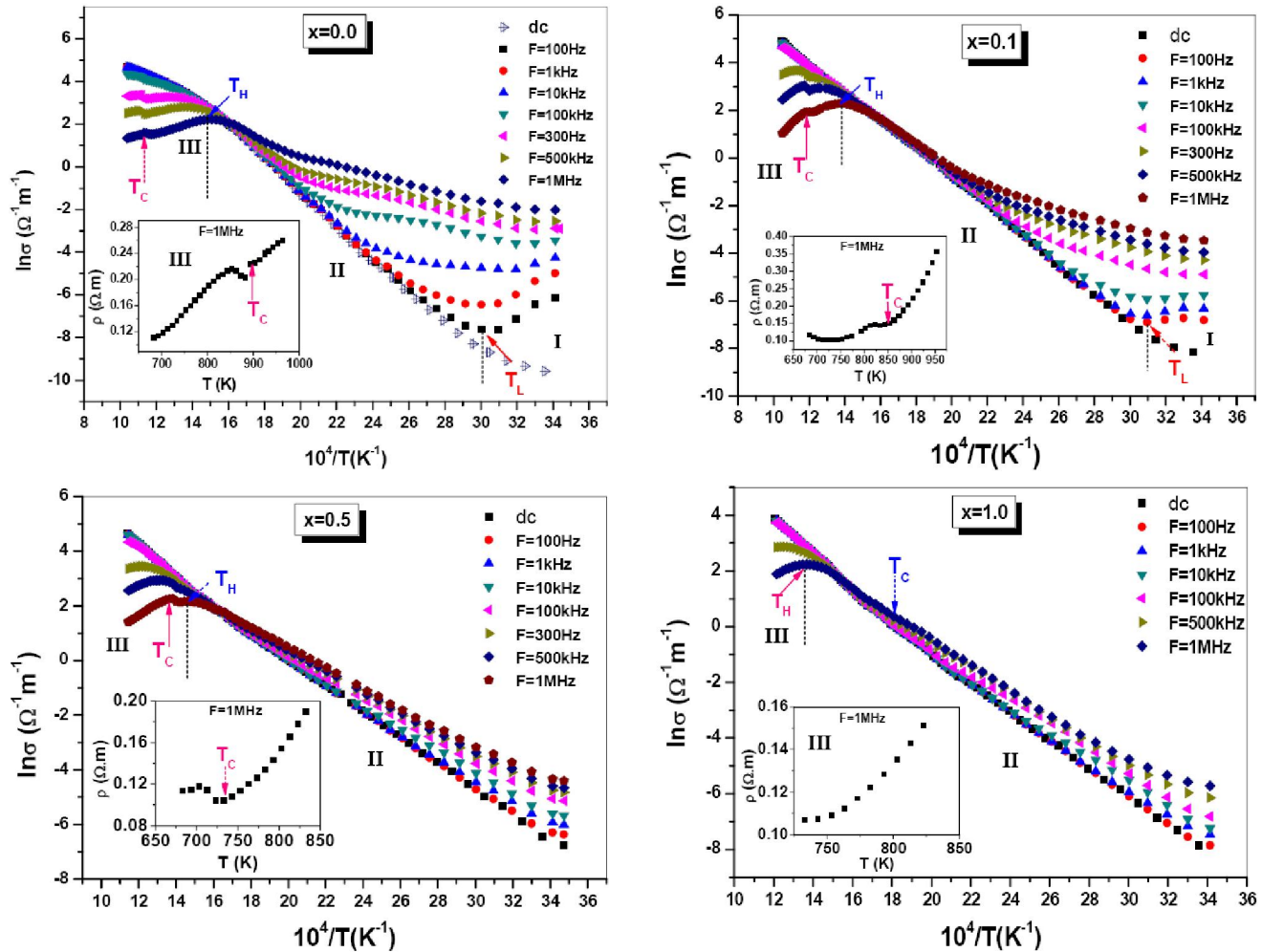


Figure 1 : Temperature dependence of dc and ac conductivities for $x = 0.0, 0.1, 0.5$ and 1.0 .

The conductivity at low temperature $T < T_L$ (region I, for $x=0.0$ and 0.1), is due to impurity and interstitial defects and it seems to be independent of temperature. This suggests that the impurity conduction plays a dominant role in this region (extrinsic region). The energy below $kT_L \approx 0.03$ eV is not sufficient for conduction mechanism. So that the conductivity seems to be independent of temperature.

In the second region II (where $T_L < T < T_H$), the conductivity increases with increasing temperature continuously with changing the slope. Just above T_L , where $T_L \approx (1/2)\theta_D$ “Debye temperature” (which was calculated from the IR spectra) the frequency dispersion of

the ac conductivity is more pronounced. In this dispersion range of region II, the activation energy E_a decreases with increasing the frequency as shown in Figure 2 for the samples of $x = 0.1, 0.3, 0.5$ and 0.9 ; as an example. This behaviour can be attributed to the ac hopping conduction of the localized carriers proposed by Pike^[18]. This model has analyzed the ac conductivity for many oxides and amorphous materials. The present results are analogous to those observed by many researchers^[19,20]. Also, it can be noticed that the activation energies associated with ac conductivity are bit lower than that the corresponding energy involved in the dc conductivity as shown in TABLE 1. For dc con-

Full Paper

ductivity the charge carriers choose the easiest path between ions, but these paths will be included some hops for which R “the distance between ions” is large. These are not important in ac conductivity. Thus rather lower activation energies may be involved in the ac conductivity than in the dc conduction.

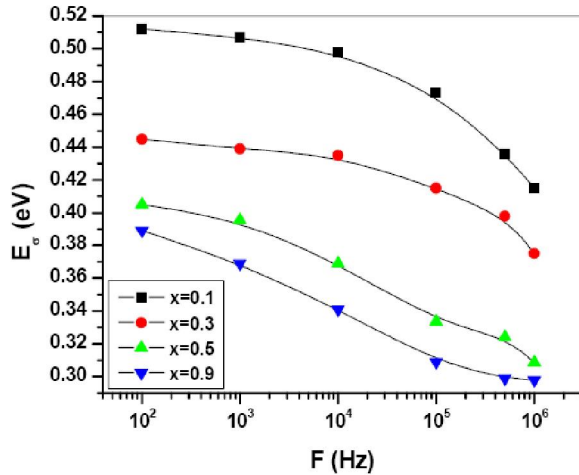


Figure 2 : The variation of the activation energy in region II with frequency.

In region III, a strange behaviour (as a metallic behaviour) has been seen at high temperature and high frequency. This metallic behaviour is shown in insets of Figure 1. According to this behaviour, the Matthiessen’s rule can be applied for the total resistivity (ρ_T):

$$\rho_T = \rho_o + \rho_{ph}(T) \tag{2}$$

where ρ_o represents the impurity defects and it is predominant in the range of $T < T_L$. While $\rho_{ph}(T)$ represents the resistivity by phonon scattering, the larger the amplitude of vibration at high temperature ($T > T_H$), the greater will be ρ_{ph} , where ρ_o can be neglected. In general, the conductivity above T_H may suffer from the electron-phonon interaction and decreasing in mobility.

In region III ($T > T_H$), it was noticed that the Curie point transition becomes more clear at high frequency especially at 500 KHz and 1 MHz. At T_C , in the metallic behaviour region $\ln \sigma$ shows a maximum value in the relation $\ln \sigma$ vs T^{-1} as shown in Figure 3. This phenomena appeared only for $x = 0.5$ (in the metallic behaviour region) and disappeared for $x > 0.5$, where the metallic behaviour is not exist. To confirm this phenomenon, the conductivity (σ) and intial permeability (μ_i) have been plotted with temperature as shown in Figure 4. T_C was determined from the maximum peak in μ_i and appeared

as a cusp in the conductivity σ at the same temperature. This behaviour may be due to the effect of eddy current at high frequency in the metallic behaviour only. The eddy current increases at high frequency and consequently increases the resistivity. But in the semiconducting region, the ferrite is characterized by low eddy current and it is not effective.

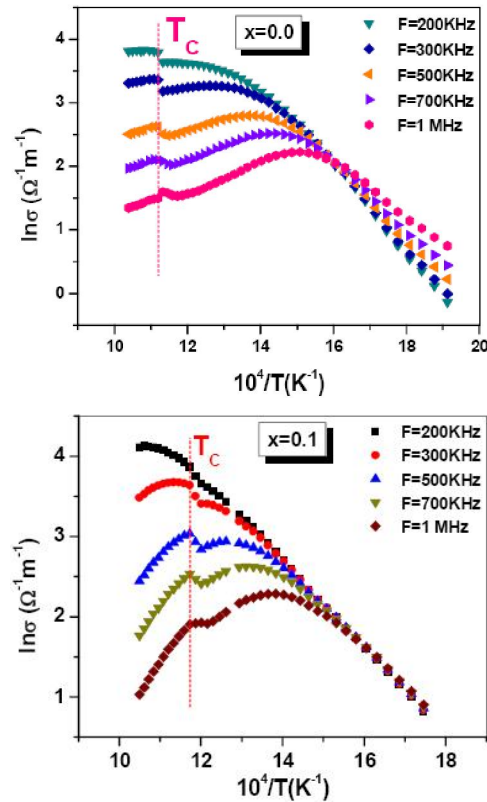


Figure 3 : The influence of frequency on the transition at Curie temperature.

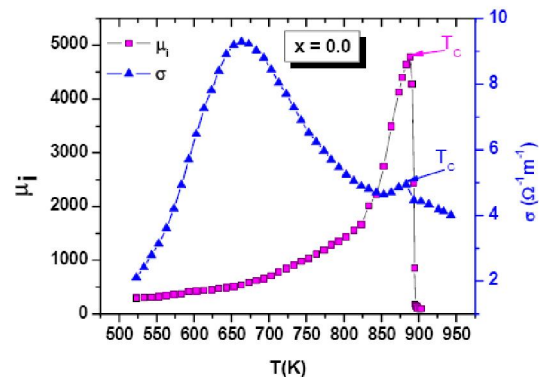
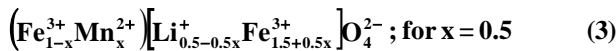


Figure 4 : A comparison between the estimated values of Curie temperature from initial permeability and conductivity measurements.

The conduction mechanism in ferrites is quite different from that in semiconductors. In ferrites the tem-

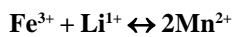
perature dependence of mobility affects the conductivity and the carrier concentration is almost unaffected by temperature variation (where n is of the order 10^{22} cm^{-3})^[21]. In ferrites the charge carriers are localized at the magnetic ions. Conduction is due to exchange of the 3d-electrons (localized at the metal ions) from Fe^{3+} to Fe^{2+} ^[22]. The compositional dependence of the electrical conductivity ($\ln \sigma$ vs. x) at room temperature at different frequencies is shown in Figure 5. It is observed that $\ln \sigma$ increases up to $x=0.5$ then decreases with further addition of Mn content. In the present series of ferrites, the cation distribution could be assumed to be:



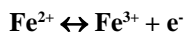
and



where y is a small fraction of Mn^{2+} ions not exceed than 20%^[23]. According to this distribution, the iron ions Fe^{3+} and Li^{1+} are replaced with Mn^{2+} ions according to:



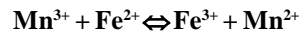
Firstly for $x = 0.5$, hopping of electron can occur between multiple valance iron ions:



localized at B-sites. The formation of Fe^{2+} ions may be due to partial evaporation of Li^{1+} ions during sintering at high temperature and they preferably occupy the B sites^[24]. Therefore, the increase of the cation parameter x is associated with the increase of Fe^{3+} content. As a consequence the probability for hopping conduc-

tion between $\text{Fe}^{2+} \leftrightarrow \text{Fe}^{3+}$ increases. Consequently, the conductivity increases for $x=0.5$.

Then for $x > 0.5$, according to the proposed cation distribution the substitution of Mn^{2+} in place of Fe^{3+} on the B-site reduces the Fe^{2+} concentration, and may be explained by the following reaction:



The electron hopping energy between $\text{Mn}^{3+} \leftrightarrow \text{Mn}^{2+}$ is larger than that between $\text{Fe}^{3+} \leftrightarrow \text{Fe}^{2+}$ ^[25]. By increasing the replacement of Fe^{3+} with Mn^{2+} ions, the numbers of ferrous and ferric ions at B-sites decrease. As the concentration of Fe^{2+} ions at B-sites are reduced, thereby the electron exchange is suppressed in terms of a model of electron hopping. Therefore, the electrical conductivity decreases for $x > 0.5$.

Figure 6 represents the variation of the activation energy in region II (ferrimagnetic region), as a function of composition x at $F=0$ Hz, 100 Hz, 1 KHz and 10 KHz for the studied ferrite system. From this figure, substituting Mn^{2+} in place of Fe^{3+} in the lattice leads to decrease E_g from 0.68 eV at $x=0.0$ to 0.41 eV at $x=0.5$, and after that the activation energy becomes approximately constant. The value of E_g for $x=0.0$ (0.68 eV) is due to a formation of small polaron hopping^[26]. While the activation energy of Li-Mn ferrite for $x = 0.3$ in the range of 0.40 ± 0.01 eV. This value is due to electron hopping. The high values of the activation energy (for $x=0.0$ and 0.1) are due to the half filled Mn^{2+} (d-orbitals) which having much lower energy and being more contracted than the Fe^{3+} orbitals. The overlapping of

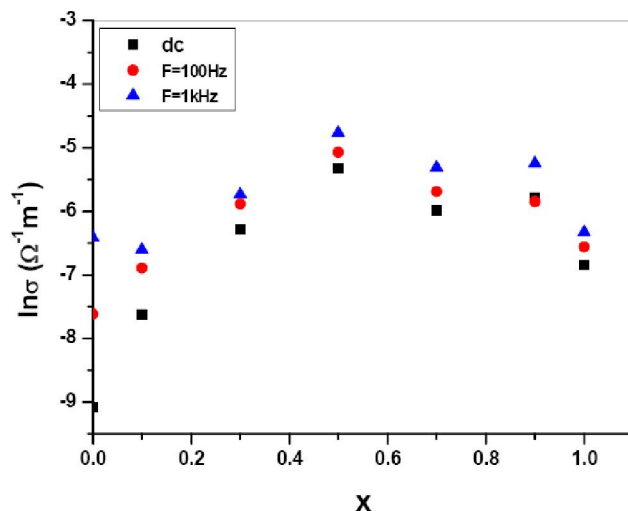


Figure 5 : Dependence of ($\ln \sigma$) on composition x at 320K at different frequencies.

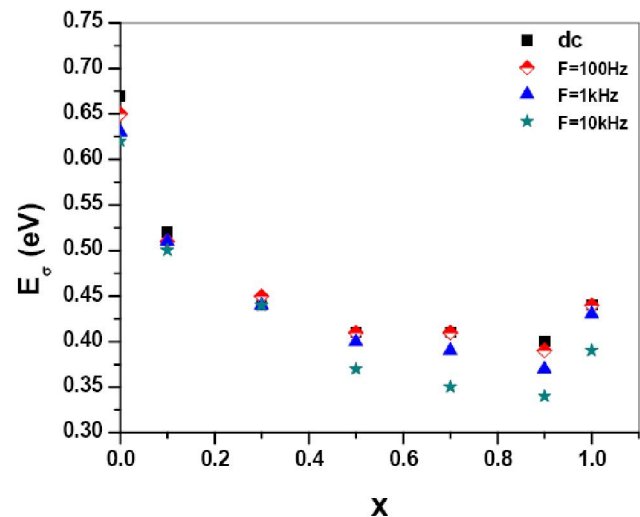


Figure 6 : The variation of the activation energy E_g with composition x at different frequencies.

Full Paper

d-orbitals of Mn^{2+} and Fe^{3+} with the 2p of the oxygen has an indirect effect on the hopping process at B-sites^[27]. When the interaction between electrons and phonons is strong, a small polaron will be formed. Further, in oxides of the iron group metals, especially in ferrites, the overlap of 3d-wave functions between neighbouring metal ions is relatively small^[21]. As such it may be assumed that the conduction mechanism for $x = 0.0$ and 0.1 may be due to hopping of small polarons. While by substituting Mn^{2+} in place of Fe^{3+} ($x > 0.1$) leads to reducing the formation of small polaron hopping until the conduction mechanism becomes due to electron hopping at high concentration of Mn ions.

Dielectric properties

The variation of the loss tangent $\tan \delta$ and dielectric constant ϵ' with temperature at different frequencies in the range from 100 Hz up to 1 MHz are represented in Figure 7 a-b for the above investigated composition of Li-Mn ferrite ($x=0.0, 0.5$ and 1.0 are presented as examples). It is observed that the $\tan \delta$ curves show an abnormal dielectric behaviour (i.e. peaks) at elevated temperature. By increasing temperature, $\tan \delta$ begins to increase slowly until it attains a maximum value and then decrease with increasing the temperature. The temperature corresponding to the peaks (T_m) was found to be shifted to lower temperature with increasing the

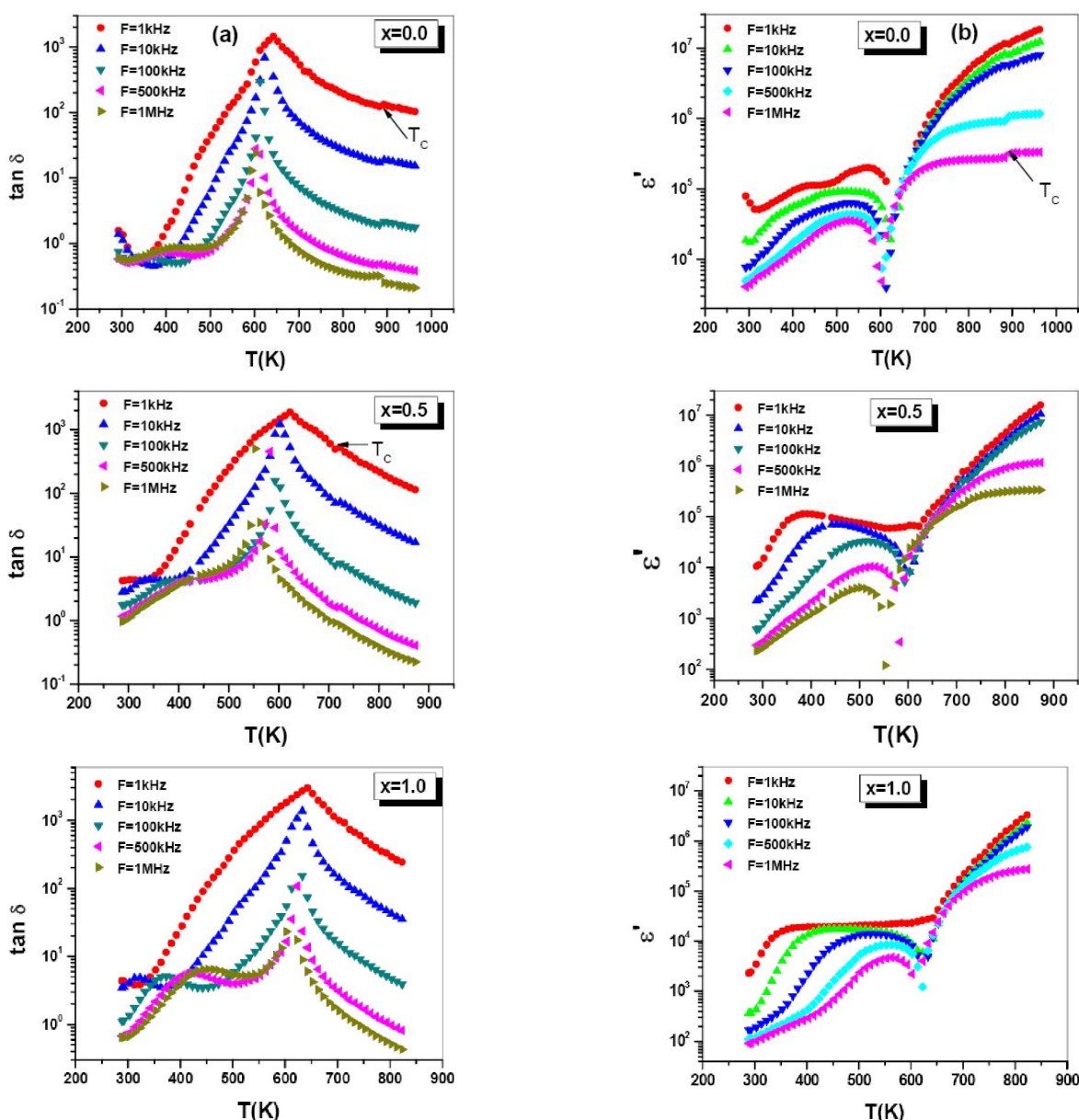


Figure 7 : Temperature dependence of (a) dielectric loss tangent $\tan(\delta)$ and (b) dielectric constant ϵ' for $x = 0.0, 0.5$ and 1.0.

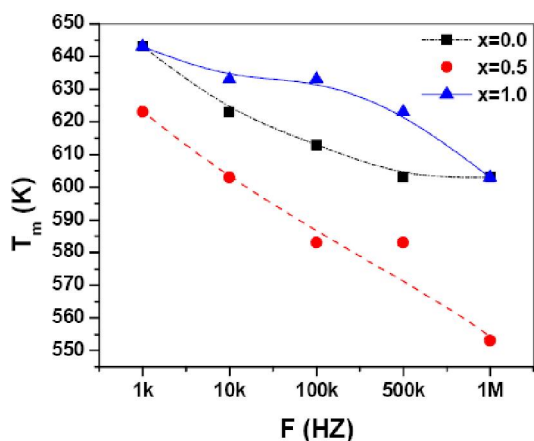


Figure 8 : The variation of T_m with frequency for the samples $x = 0.0, 0.5$ and 1.0 .

frequencies as shown Figure 8. From the relationship of ϵ'' versus temperature, Figure 7b, it can be noticed that more than one inverse peak is obtained. The inverse peak is corresponding to the maximum in $\tan \delta$ where $\tan \delta = \epsilon''/\epsilon'$, where ϵ'' is the imaginary part of the complex dielectric constant, which describes the dissipation energy, and ϵ' is the real part, which describes the stored energy. The maximum in $\tan \delta$ is due to the rapid decrease in ϵ' as the frequency increases through the dispersion. These behaviours of the dielectric properties of the investigated compounds of Li-Mn ferrite depend on the polarization of the system. Consequently, the electron exchange between Fe^{2+} and Fe^{3+} ions, and hole transfer ($\text{Mn}^{2+} \leftrightarrow \text{Mn}^{3+}$) at octahedral sites are responsible for the electric conduction in this ferrite, where the local displacements of localized electric charge carriers include dielectric polarization in ferrites. On increasing the temperature, the electrical conductivity increases due to the increase in thermally activated drift mobility of electric charge carriers according to the hopping conduction mechanism. Therefore, the dielectric polarization increases causing a marked increase in $\tan \delta$ as the temperature increase up to the peak values. At the resonance, where the applied frequency becomes equal to that of the ions, a relaxation peak appears, varying in position and shape depending on the Mn^{2+} concentration for the compositions. After the relaxation peak and by increasing the temperature, $\tan \delta$ decreases until it reaches a flat region which observed clearly at high frequency. In the first region (before the peaks) the low frequency and low temperature helps in the aligning the dipoles in the field

direction with the result of an increase in polarization as well as $\tan \delta$. Also, as the temperature increases the thermal energy liberates more localized dipoles and the field tries to align them in its direction either by rotational or orientational contributing to an increase in $\tan \delta$ up to a peak value. In the second region (after the peaks) the temperature becomes relatively high and the dipoles were distributed with the result of decrease in $\tan \delta$ ^[28]. As the temperature increases (in the flat region) the disorder becomes maximum. Moreover, the mobility of holes is smaller than that of electrons and the replacement of Fe^{3+} with Mn^{2+} in Li-Mn ferrite decreases the number of charge carriers which means the more contribution of p-carriers to polarization will appear at high concentration of Mn^{2+} ions and high temperatures. Also the shift of relaxation dielectric peak towards lower temperature with increasing frequency for the studied composition may be due to the decrease in the hopping frequency for both types of charge carriers with increasing temperature.

CONCLUSION

- 1 The conduction mechanism was discussed through small polaron hopping model for $x=0.0$ and 0.1 but for $x=0.3$, the conduction mechanism is due to the electron hopping.
- 2 At high temperature, high frequency in the ac conductivity, an abnormal behavior (as a metallic behaviour) is appeared. This result may be related to the effect of eddy current.
- 3 The dielectric behaviour can be explained in terms of the electron exchange between Fe^{2+} and Fe^{3+} , and the hopping of a hole between Mn^{2+} and Mn^{3+} ions at B sites, suggesting that the polarization in these compounds is similar to that of the conduction process in ferrites.
- 4 Abnormal behaviour (peaks) was observed in the $\tan \delta$ curves at relatively high temperatures. Such relaxation peaks occur when the jumping frequency of localized electrons between Fe^{2+} and Fe^{3+} equals that of the applied AC electric field.

REFERENCES

- [1] V.G.Patil, Sagar E.Shirsath, S.D.More, S.J.Shukla, K.M.Jadhav; Journal of Alloys and Compounds, **488**, 199-203 (2009).

Full Paper

- [2] Yang Bai, Ji Zhou, Zhilun Gui, Zhensheng Yue, Longtu Li; Materials Science and Engineering, **B99**, 266 (2003).
- [3] J.R.Dahn, U.Vom Sacken, C.A.Michal; Solid State Ionics, **44**, 87 (1990).
- [4] S.Akhter, M.A.Hakim; Mater.Chem.and Phys., **120**, 399 (2010).
- [5] J.Darul, W.Nowicki, P.Piszora, C.Baetz, E.Wolska; Journal of Alloys and Compounds, **401**, 60-63 (2005).
- [6] Seema Verma, P.A.Joy; Materials Research Bulletin, **43**, 3447-3456 (2008).
- [7] Vivek Verma, Vibhav Pandey, Sukhveer Singh, R.P.Aloysius, S.Annapoorani, R.K.Kotanala; Physica, **B404**, 2309-2314 (2009).
- [8] Alex Goldman; Modern Ferrite Technology, Marcel Dekker, New York, (1993).
- [9] O.Yuqiu, Y.Haibin, Y.Nan, F.Yuzun, Z.Hongyang, Z.Guangtian; Mater.Lett., **60**, 3548-3552 (2006).
- [10] K.S.Rao, P.M.Krishna, D.M.Prasad, D.Gangadharudu; J.Mater.Sci., **42**, 4801 (2007).
- [11] S.A.Safan, A.S.Seoud, R.A.El-Shater; Phys., **B365**, 27-42 (2005).
- [12] Y.M.Z.Ahmed; Ceramics International, **36**, 969 (2010).
- [13] M.Goodarz Naseri, E.Bin Saion, H.Abbastabar Ahangar, M.Hashim, A.H.Shaari; J.Mag.and Mag. Mater., **323**, 1745 (2011).
- [14] S.A.Mazen, B.A.Sabrah; Thermochemica.Acta, **105**, 1 (1986).
- [15] R.G.Kharabe, R.S.Devan, B.K.Chougale; Journal of Alloys and Compounds, **463**, 67-72 (2008).
- [16] S.A.Mazen, S.F.Mansour, T.A.Elmosalami, H.M.Zaki; J.of Alloys and Compounds, **472**, 307-313 (2009).
- [17] Ibetombi Soibam, Sumitra Phanjoubam, L.Radhapiyari; Physica, **B405**, 2181-2184 (2010).
- [18] G.F.Pike; Phys.Rev., **B1572**, 6 (1972).
- [19] M.Suzuki; J.Phys.Chem.Solids, **41**, 1253-24 (1980).
- [20] S.A.Mazen, et al.; J.Physica D: Appl.Phys., **30**, 1799 (1997).
- [21] B.Viswanathan, V.R.R.Murthy; Ferrite Materials, Science and Technology, Norsa Publishing House, (1990).
- [22] A.J.Bosmann, C.C.Creve; Phys.Rev., **144**, 763 (1956).
- [23] P.P.Hankare, R.P.Patil, U.B.Sankpal, S.D.Jadhav, P.D.Lokhande, K.M.Jadhav, R.Sasikala; J.of Sol. Stat.Chem., **182**, 3217-3221 (2009).
- [24] Radhapiyari et al.; Mat.Lett., **44**, 65-69 (2000).
- [25] B.Ramesh, D.Ravinder; Materials Letters, **62**, 2043-2046 (2008).
- [26] M.I.Kliger; Phys.Status Solidi, **B79**, 9 (1977).
- [27] J.A.Kulkarni, K.Muraleedharan, J.K.Srivastava, V.R.Marathe, V.S.Darshane, C.R.K.Murthy, R.Vijayaraghavan; J.Phys.C: Solid State Phys., **18**, 2593 (1985).
- [28] M.R.Anantharanan, S.Sincthu, S.Tagatheesan, K.A.Molini, Kurian; J.Phys.D: Appl.Phys., **32**, 1801 (1999).